BREAST

Vascular characterisation of triple negative breast carcinomas using dynamic MRI

**Sonia P. Li · Anwar R. Padhani · N. Jane Taylor · Mark J. Beresford ·
Mei-Lin W. Ah-See · J. James Stirling · James A. d'Arcy · David J. Collins ·
Andreas Makris**

Abstract

Objectives Triple-negative (ER-/PR-/HER2-) breast carcinomas (TNBC) are aggressive tumours with underexplored imaging features. This study investigates whether their vascular characteristics as assessed by dynamic contrast-enhanced (DCE) and dynamic susceptibility contrast-enhanced (DSC) MRI are distinct from the prognostically more favourable ER+/PR+/HER2- cancers.

Methods Patients with primary breast cancer underwent MRI before neoadjuvant chemotherapy and were identified as ER-/PR-/HER2- or ER+/PR+/HER2- from core biopsy specimens. MRI parameters reflecting tissue perfusion, permeability, and extracellular leakage space were measured. Values for inflow transfer constant (K^{trans}), outflow rate constant (k_{ep}), leakage space (v_e), area under the gadolinium curve ($IAUGC_{60}$), relative blood volume (rBV) and flow (rBF), and Mean Transit Time (MTT) were compared across receptor status and with known prognostic variables.

Results Thirty seven patients were assessable in total (16 ER-/PR-/HER2-, 21 ER+/PR+/HER2-). Lower v_e ($p=0.001$), shorter MTT ($p=0.007$) and higher k_{ep} values ($p=0.044$) were observed in TNBC. v_e was lower across all T stages, node-negative ($p=0.004$) and low-grade TNBC ($p=0.037$). v_e was the best predictor of triple negativity (ROC AUC 0.80).

Conclusions TNBC possess characteristic features on imaging, with lower extracellular space (higher cell density) and higher contrast agent wash-out rate (higher vascular permeability) suggesting a distinctive phenotype detectable by MRI.

Keywords Magnetic resonance imaging · Functional · Breast neoplasms · Angiogenesis · Pathological · Triple negative breast cancers · Permeability

Abbreviations

bFGF	Basic fibroblast growth factor
CALGB	Cancer and Leukemia group B
DCE-MRI	Dynamic contrast-enhanced MRI
DSC-MRI	Dynamic susceptibility contrast-enhanced MRI
ECM	Extracellular matrix
ER	Oestrogen receptor
FISH	Fluorescence in-situ hybridisation
Gd-DTPA	Gadopentetate dimeglumine
HER2	Human epidermal growth factor receptor-2
$IAUGC_{60}$	Initial area under the gadolinium curve after the first 60 s
k_{ep}	Outflow rate constant
K^{trans}	Inflow transfer constant
MRI	Magnetic resonance imaging

S. P. Li (✉) · M. J. Beresford · M.-L. W. Ah-See · A. Makris
Academic Oncology Unit, Mount Vernon Cancer Centre,
Northwood, Middlesex HA6 2RN, UK
e-mail: soniali@gmail.com

A. R. Padhani · N. J. Taylor · J. J. Stirling
Paul Strickland Scanner Centre, Mount Vernon Hospital,
Northwood, Middlesex HA6 2RN, UK

J. A. d'Arcy · D. J. Collins
CR UK and EPSRC Cancer Imaging Centre, Royal Marsden NHS
Foundation Trust and Institute of Cancer Research,
Sutton, Surrey SM2 5PT, UK

MTT	Mean transit time
NAC	Neoadjuvant chemotherapy
PET-CT	Positron emission tomography-computed tomography
PR	Progesterone receptor
rBF	Relative blood flow
rBV	Relative blood volume
ROC	Receiver operating curve characteristic
TE	Echo time
TNBC	Triple-negative breast carcinomas
TNM	Tumour, node, metastasis
TR	Repetition time
v_e	Leakage space
VEGF	Vascular endothelial growth factor

Introduction

Triple-negative breast carcinomas (TNBC) have been shown to be a distinct entity displaying aggressive features, both biologically and clinically [1]. These tumours are typically oestrogen receptor (ER)-negative, progesterone receptor (PR)-negative and lack the over-expression or amplification of human epidermal growth factor receptor (HER2) and hence therapeutic options other than cytotoxic treatments are often limited. They account for between 10% and 20% of all breast cancer patients but patients with this phenotype tend to fare worse prognostically, with shorter disease-free and overall survival [2]. Although this may be accounted for by the paucity of suitable treatments, it has been suggested that triple-negative breast cancers are themselves a separate biological disease [1]. Gene expression profiling has identified five major molecular subtypes of breast cancer: luminal A and B (both ER+), normal breast-like, basal-like and HER2+ (all ER-) [3–5]. Although most TNBC possess a basal phenotype, they are not synonymous with basal-like breast cancers, with a discordance of up to 30% described in the literature [2, 6]. Their behaviour is contrary to that of the more favourable prognostic group of ER+/PR+/HER2- breast cancers.

Functional magnetic resonance imaging techniques such as dynamic contrast-enhanced (DCE) and dynamic susceptibility contrast (DSC)-enhanced MRI have the ability to document tumour vascularisation and interrogate the extracellular extravascular space, with particular MRI-derived parameters reflecting different aspects of the tumour microenvironment [7]. These non-invasive methods are particularly attractive with regard to being able to probe the vascularity of triple-negative breast cancers and to identify potential biological markers suitable for specific targeted therapies. Previous imaging studies have evaluated the morphological and metabolic characteristics of TNBC in

comparison with ER+/PR+/HER2 cancers with both MRI and PET-CT respectively, but as far as we aware, there is a relative lack of data regarding both the tumour stromal environment and the vasculature [8, 9].

The purpose of this study was to investigate whether breast cancers displaying the triple-negative phenotype exhibit unique vascular characteristics compared with the more common and prognostically more favourable ER+PR +HER2- group, and to quantify these differences using DCE-MRI and DSC-MRI.

Materials and methods

Study design

Eighty-three women (median age 46 years; range, 26–72) with newly diagnosed, histologically-proven primary breast cancer underwent MRI before neoadjuvant chemotherapy (NAC) as part of two prospective studies investigating the role of MRI in response to NAC [10]. All research was performed in accordance with the Helsinki Declaration. Approval was sought from the local institutional ethics review board (West Hertfordshire Hospitals protocol number EC2001-26) and informed consent obtained from all patients. We retrospectively identified ER-/PR-/HER2- or ER+/PR+/HER2- cancer cohorts from pre-treatment core biopsy specimens. Clinical staging at diagnosis was performed in accordance with the TNM (Tumour, Node, Metastasis) staging classification of malignant tumours as described by the International Union against Cancer Criteria [11].

Histopathological scoring of hormone and HER2 receptor status

Histological information was acquired from pre-treatment, diagnostic core biopsy specimens and graded according to the Bloom-Richardson scoring system [12]. Low and moderate grade tumours were grouped together as there were too few low-grade lesions for analysis. Oestrogen receptor (ER) and progesterone receptor (PR) scoring was performed according to the Allred score, a composite of the percentage of cells that stained (scored from 0 to 5) and the intensity of their staining (rated as 1–3), using immunohistochemical methods [13]. The threshold for hormone receptor positivity was taken as a composite score of 3 and above. HER2 (human epidermal growth factor receptor) status was deemed to be positive if 3+ and negative if 0 or 1+ on immunohistochemistry. Tumours which were 2+ were sent for further testing and classified as positive if amplified (≥2.1 copies) on FISH (fluorescence in-situ hybridisation) testing.

MRI data acquisition and analysis

The MRI examinations were performed on a 1.5 T Siemens Symphony (Siemens Medical Systems, Erlangen, Germany) using a dedicated bilateral breast coil. Initial diagnostic coronal and axial T_1-weighted and T_2-weighted MRI were obtained through both breasts. Proton density-weighted gradient recalled echo images were acquired sagittally (TR 350 ms, TE 4.7 ms, flip angle (α) 6°) for four slices (three through tumour and one through the contralateral normal breast). Dynamic T_1-weighted (relaxivity-weighted) images (TR 11 ms, TE 4.7 ms, α 35°, 256×256 matrix) matched to the proton density images were then acquired at the same slice positions every 12 s for a total imaging time of 8 min (40 sets) for the purposes of T_1 mapping [14, 15]. Intravenous gadopentetate dimeglumine [0.1 mmol/kg body weight Gd-DTPA, Magnevist, Bayer-Schering] was injected at 4 ml/s during the fifth acquisition time point followed by a 20 ml saline flush at 4 ml/s. Dynamic T_2*-weighted (susceptibility-weighted) images (TR 30 ms, TE 20 ms, (α) 40°, 128×128 matrix, central slice) using 0.2 mmol/kg IV Gd-DTPA injected at 4 ml/s after 20 s, were then acquired every 2 s over 2 min (60 sets).

Images were analysed using specialist MRI software (MRIW version 4.3, Institute of Cancer Research, London, UK) [16] with whole tumour regions of interest (ROI) drawn on DCE-MRI T_1-weighted subtraction images by a single observer. DCE-MRI analysis was performed using pharmacokinetic modelling of contrast kinetics according to the 2-compartment Tofts model [17] and a modified Fritz-Hansen assumed arterial input function [18–20]. Values for quantitative kinetic parameters K^{trans} (inflow transfer constant; min^{-1}), v_e (leakage space; %), k_{ep} (outflow rate constant; min^{-1}) and semi-quantitative parameter $IAUGC_{60}$ (initial area under the gadolinium-time curve over 60 s; mM/s^{-1}) as well as T_2*-weighted quantitative parameters rBV (relative blood volume; arbitrary units (AU)), MTT (mean transit time; s) and rBF (relative blood flow; AU) were calculated pixel-by-pixel.

K^{trans} is a transfer constant measuring the rate of transport of contrast medium from plasma to the extravascular extracellular space (EES) and provides a measure of vascular permeability and blood flow; v_e is the fraction of the tumour volume occupied by the EES, whilst k_{ep} describes the outflow rate of contrast medium from the EES back to plasma. These parameters are related by the equation:

$$k_{ep} = K^{trans}/v_e$$

Dynamic T_2*-weighted parameters are derived from the changing tissue signal intensities corresponding to the first passage of a bolus of contrast agent in the vascular space

[16]. By fitting a gamma variate model function, relative blood volume (rBV), mean transit time (MTT) and relative blood flow (rBF) can be measured. MTT is the mean time for contrast agent to perfuse a region of interest. According to tracer dilution theory, rBV is the area under the fitted curve and MTT is the full width half maximum of the fitted peak, with these constants related by the following central volume theorem:

$$BF = BV/MTT$$

Statistical analysis

Statistical analysis was performed using the StatsDirect software package (Sale, Cheshire, UK). Median values for baseline parameters were calculated from pixel histograms of kinetic parameters because of their non-normal distributions. MRI-derived kinetic parameters were compared across receptor status and with other known prognostic variables (age, grade, tumour stage, nodal status) using the Mann-Whitney U test. Analysis of Receiver Operating Characteristic (ROC) curves for each parameter was used to elucidate the parameter best able to identify the triple-negative phenotype.

Results

In total, 37 patients were suitable for analysis, 16 of whom were identified as ER-/PR-/HER2- and 21 as ER+/PR+/HER2-. 12 patients did not undergo their first MRI, one patient's tumour was not visible on MRI, full receptor status was not available in 11 and 22 patients with other receptor phenotypes were excluded. TNBC comprised 19% of the total study population with a median age of 42.5 years (range 34–57) and median tumour size of 60 mm (range 40–100), with most being of the invasive ductal subtype (88%). In comparison, in the ER+/PR+/HER2- group, the median age was 49 years (range 26–70) and median tumour size 50 mm (range 25–150) with 71% exhibiting ductal histology. There were significantly more high-grade tumours in the TNBC group ($p=0.006$). The characteristics of each group are provided in Table 1.

Overall significantly higher values for k_{ep} (0.70 vs 0.56, $p=0.044$), and lower values for v_e (0.33 vs 0.39, $p=0.001$) and MTT (44.27 vs 47.69, $p=0.007$) were observed in TNBC (Table 2; Fig. 1). Both rBV and rBF were higher in TNBC but these results were not statistically significant. ROC curve analysis revealed v_e to be the best identifier of triple negativity (sensitivity 81%, specificity 76%, area under ROC curve 0.80). Representative images with corresponding histograms comparing v_e and k_{ep} in TNBC with ER+/PR+/HER- are shown in Fig. 2.

Table 1 Characteristics of ER-/PR-/HER2- and ER+/PR+/HER2- patient groups

Patient/disease characteristics	ER-/PR-/HER2- (n=16)	ER+/PR+/HER2- (n=21)	Significance of difference
Median age (years)	42.5	49	p=0.192
Histology			
IDC	14	15	χ^2=1.384
ILC	2	6	df=1
			p=0.239
Median tumour size (mm)	60	50	p=0.050
Clinical T stage:			
T2	5	13	χ^2=5.57
T3	9	4	df=2
T4	2	4	p=0.062
Clinical nodal status:			χ^2=1.046
Positive	8	7	df=1
Negative	8	14	p=0.306
Grade:			
1	0	2	χ^2=12.314
2	4	13	df=3
3	12	4	p=0.006
N/A	0	2	

ER oestrogen receptor, *PR* progesterone receptor, *HER2* human epidermal growth factor receptor, *IDC* invasive ductal carcinoma, *ILC* invasive lobular carcinoma, *df* degrees of freedom

[a] χ^2 chi-square test

No correlation was found between age and any MRI kinetic parameters. When stratified according to tumour grade within each cohort, k_{ep} values were higher in high-grade lesions compared with low-grade TNBC (0.82 vs 0.51, p=0.019) as were rBV (276.14 vs 79.25, p=0.008) and rBF (6.16 vs 1.87, p=0.014) (Table 3) but not within ER+/PR+/HER2- cancers. Comparisons were also made between TNBC and ER+/PR+/HER2- groups. Values for v_e (0.33 vs 0.40, p=0.037) and MTT (40.49 vs 47.55, p=0.008) remained significantly lower but only in low-grade TNBC. This effect was not seen in high-grade tumours (Mann-Whitney U test; p>0.05).

For tumour stage comparisons, T3 and T4 breast cancers were grouped together as there were too few T4 tumours for separate analysis. Values for v_e were significantly lower across all T stages in TNBC (T2 0.30 vs 0.38, p=0.035; T3/4 0.34 vs 0.41, p=0.012) compared with the ER+PR+HER2- group. Although values for k_{ep} were higher and MTT shorter in TNBC across all T stages, these results did not reach statistical significance.

Values for v_e were also significantly lower for node-negative TNBC (0.33 vs 0.41, p=0.004) and in node-positive breast cancer, MTT was shorter in the TNBC group (43.96 vs 47.58, p=0.008) (Table 4). k_{ep} was once again

Table 2 Comparison of dynamic MRI kinetic parameters in triple negative breast cancers with ER+/PR+/HER2- breast cancers

MRI parameters	Triple negative BC (n=16)	ER+/PR+/HER2- BC (n=21)	Mann-Whitney U test	ROC AUC (95% CI)
K^{trans}	0.19 (0.18–0.29)	0.23 (0.19–0.27)	p=0.575	0.56 (0.34–0.77)
v_e	0.33 (0.28–0.35)	0.39 (0.37–0.44)	**p=0.001**	0.80 (0.37–1.00)
k_{ep}	0.70 (0.60–0.93)	0.56 (0.48–0.66)	**p=0.044**	0.70 (0.52–0.88)
$IAUGC_{60}$	12.59 (12.13–16.13)	14.17 (12.09–16.01)	p=0.596	0.55 (0.34–0.77)
rBV	215.51 (141.77–282.33)	132.96 (119.45–257.25)	p=0.533	0.57 (0.35–0.79)
rBF	5.68 (3.33–6.33)	2.98 (2.49–5.37)	p=0.252	0.63 (0.41–0.84)
MTT	44.27 (38.31–46.13)	47.69 (45.74–49.69)	**p=0.007**	0.77 (0.31–1.00)

ER oestrogen receptor, *PR* progesterone receptor, *HER2* human epidermal growth factor receptor, *BC* breast cancer, *ROC AUC* area under the receiver operating characteristic curve

[a] 5th to 95th percentile intervals are quoted in parentheses unless otherwise stated; statistically significant values are highlighted in bold
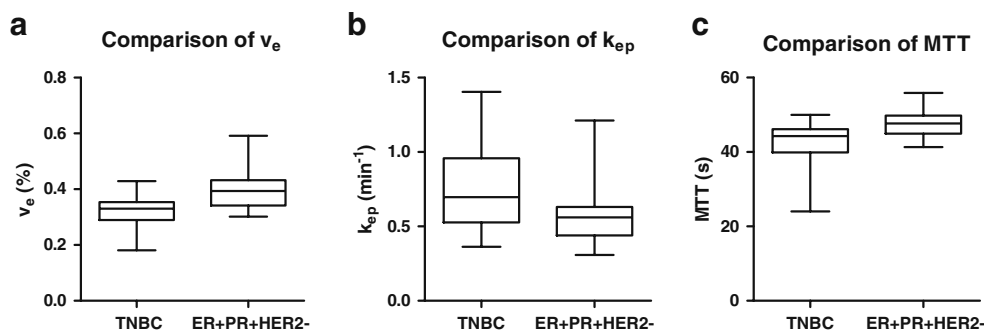
Fig. 1 Box and whisker plots of MRI kinetic parameters (median, interquartile range, 5th and 95th percentile values) illustrating significant differences between the TNBC and ER+PR+HER2- patient groups. **a** TNBC: v_e 0.33 (0.28–0.35), ER+PR+HER2-: v_e 0.39 (0.37–0.44); $p=$ 0.001. **b** TNBC: k_{ep} 0.70 (0.60–0.93), ER+PR+HER2-: k_{ep} 0.56 (0.48–0.66); $p=0.044$. **c** TNBC: MTT 44.27 (38.31–46.13), ER+PR+HER2-: MTT 47.69 (45.74–49.69); $p=0.007$

higher in the TNBC group across all nodal stages but results did not reach statistical significance.

Discussion

Triple-negative breast cancers constitute only 10% to 20% of all breast cancers but treatment is limited by the lack of effective targeted therapies and by their aggressive clinical behaviour, which is typically characterised by earlier relapses and worse outcomes [5]. The clinical characteristics of the TNBC population in this study are similar to those previously reported, in that women tend to be younger, have an increased likelihood of lymph node involvement and higher grade tumours in comparison to hormone receptor-positive, HER2 receptor-negative patients.

It is now emerging that triple-negative breast cancers have distinct clinical and pathological features. Histopathological characterisation has revealed these tumours to be of higher grade, with higher mitotic indices and Ki67 counts. Other features have included scant stromal content, central necrosis, pushing margins of invasion, a stromal lymphocytic infiltrate and multiple apoptotic cells [1, 21, 22]. Molecular profiling has revealed the differential expression of genes associated with cell division and proliferation and intracellular DNA repair between both subtypes [23]. To date, there has been a paucity of studies evaluating the functional imaging characteristics of TNBC. Studies have revealed distinct morphological features on mammography and MR imaging [8, 24–26] with fluorine-18 fluorodeoxyglucose (FDG)-positron emission tomography (PET) demonstrating a higher sensitivity in detecting these tumours because of enhanced FDG uptake [9]. Increased FDG uptake is likely to be related to upregulation of glucose transporters which may be related to constitutive or hypoxia-mediated upregulation of HIF-1 alpha [27]. Activation of HIF-1 also results in increased tumour

angiogenesis which in turn results in a chaotic tumour vascular bed with arterio-venous shunts as discussed below.

We have demonstrated lower values of v_e in TNBC with DCE-MRI, which values of v_e in TNBC, which describes the fraction of the tumour volume occupied by the EES. This is consistent with a more compact, tightly packed and a highly cellular microenvironment. Values for v_e also remained significantly lower in low-grade TNBC in comparison with ER+PR+HER2- tumours despite there being a higher number of high-grade tumours in TNBC. Although v_e was lower in high-grade TNBC in comparison with the ER+PR+HER2- arm, these results were not statistically significant which may be partly accounted for by the smaller patient numbers in the latter. Furthermore, v_e was reduced in the triple-negative phenotype for all T stages and node-negative patients. Although this was not seen in the node-positive population, lymph node positivity, a reflection of a more aggressive primary breast tumour and corresponding underlying tumour hypercellularity, may be an overriding influence over hormonal and HER2 status on v_e values.

In preclinical breast cancer models, tumour-derived fibroblasts in the stroma are able to induce greater cell proliferation because of higher basic fibroblast growth factor (bFGF) levels in hormone receptor-negative tumours. Gene expression profiling has also revealed that stromal expression can vary amongst breast carcinomas, as it is dependent on the differential expression of a set of extracellular matrix-related (ECM 1-4) genes [28]. ECM1 tumours were overrepresented by basal-like tumours and highly associated with lymphoid infiltration, which in turn, can stimulate fibroblastic production of matrix components [28]. Furthermore, patients with an ECM1 tumour profile had worse outcomes suggesting that stromal composition may be a factor in the poorer prognosis of TNBC.

Preclinical evidence supports not only increased cellularity but also increased neovascularisation in TNBC [29]. Greater intratumoural levels of the angiogenic mediator, VEGF (vascular endothelial growth factor) have been

Fig. 2 Representative parametric maps with corresponding whole tumour histogram depictions of: **a** lower v_e values in (*i*) TNBC compared with (*ii*) ER+/PR+/HER2- BC **b** higher k_{ep} values in (*i*) TNBC compared with (*ii*) ER+/PR+/HER2- BC in two patients matched for tumour size (T2), lymph node status (N0), grade (G3) and histological subtype (invasive ductal carcinoma)
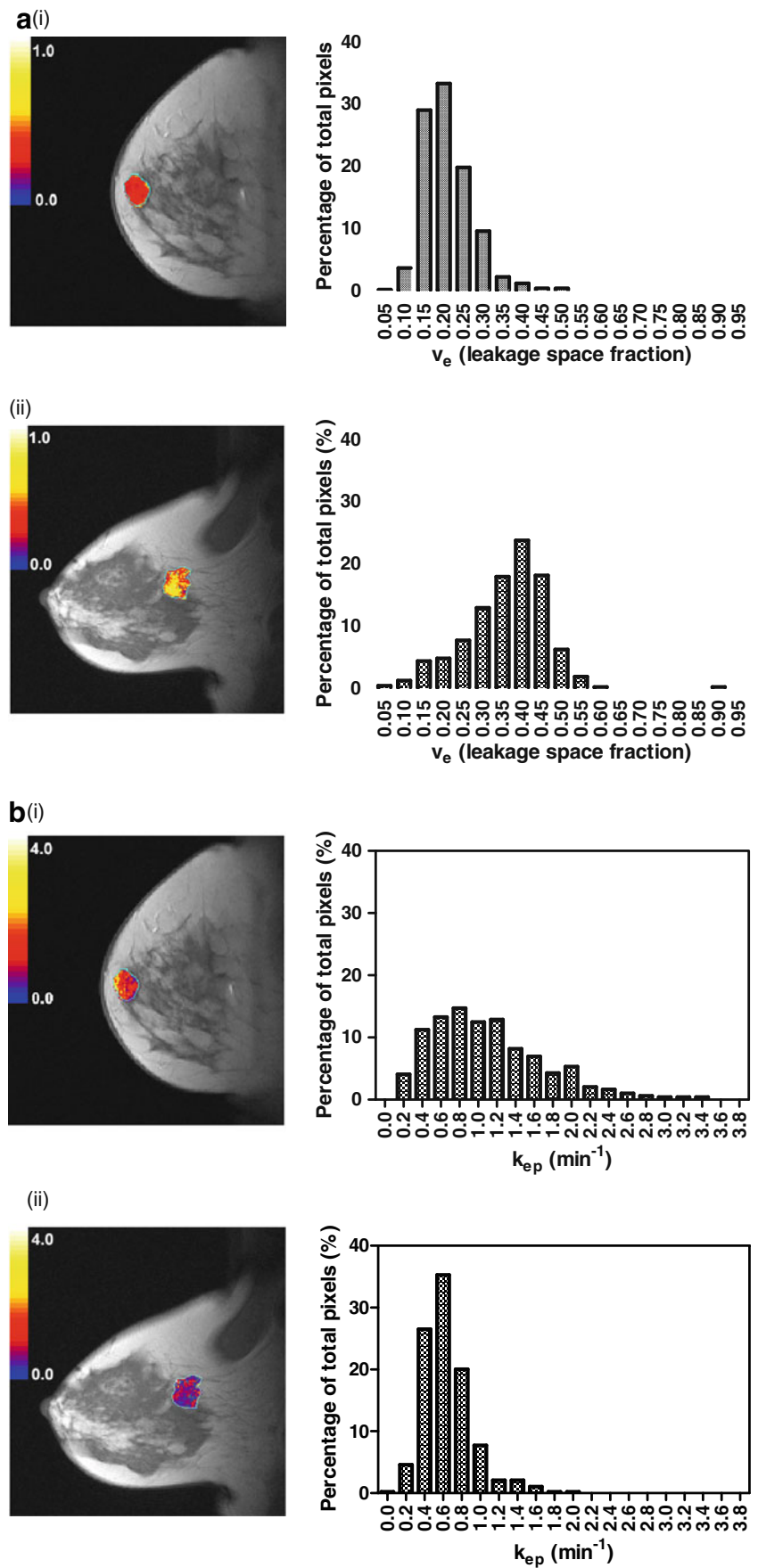
MRI parameters	Grade	Triple negative BC	ER+/PR+/HER2-	p-value[a]
K^{trans}	Low	0.16	0.22	0.062
	High	0.21	0.24	0.953
	p-value[b]	0.058	0.665	
v_e	Low	0.33	0.40	**0.037**
	High	0.32	0.37	0.212
	p-value[b]	0.860	0.736	
k_{ep}	Low	0.51	0.55	0.885
	High	0.82	0.60	0.133
	p-value[b]	**0.019**	0.357	
$IAUGC_{60}$	Low	11.41	14.17	0.080
	High	13.64	14.60	0.862
	p-value[b]	0.058	0.665	
rBV	Low	79.25	143.80	0.142
	High	276.14	200.20	0.540
	p-value[b]	**0.008**	0.945	
MTT	Low	40.49	47.55	**0.008**
	High	45.07	47.71	0.188
	p-value[b]	0.106	0.945	
rBF	Low	1.87	2.99	0.240
	High	45.07	47.71	0.188
	p-value[b]	**0.014**	0.945	

MRI parameters	Nodal status	TNBC	ER+/PR+/HER2-	p value[a]
K^{trans}	N0	0.18	0.23	0.127
	N+	0.20	0.18	0.281
	p value[b]	0.328	0.110	
v_e	N0	0.33	0.41	**0.004**
	N+	0.33	0.32	0.463
	p value[b]	0.721	0.025	
k_{ep}	N0	0.70	0.56	0.441
	N+	0.73	0.56	0.121
	p value[b]	0.442	0.636	
$IAUGC_{60}$	N0	12.19	14.38	0.145
	N+	12.91	13.14	0.336
	p value[b]	0.505	0.197	
rBV	N0	169.79	154.63	>0.999
	N+	261.23	102.22	0.230
	p value[b]	>0.999	0.177	
MTT	N0	44.46	47.69	0.151
	N+	43.96	47.58	**0.024**
	p value[b]	0.620	0.950	
rBF	N0	5.50	3.01	0.724
	N+	5.87	2.18	0.1091
	p value[b]	0.805	0.177	

reported, with levels up to three times greater than that seen in ER+/PR+ tumours [30]. Other studies have reported p53 mutations in up to 80% of TNBC compared with 20% in other breast cancers, which are associated with higher plasma and intratumoural VEGF levels [31, 32]. Wild-type p53 downregulates the VEGF promoter and is involved in the regulation of thrombospondin-1, an inhibitor of angiogenesis. Higher bFGF levels have also been implicated in increased angiogenesis via VEGF upregulation in breast cancer cells [33]. The consequent hypervascularisation results in structurally and functionally abnormal tumour vessels, multiple arterio-venous shunts and loss of blood flow regulation [34]. In this study, the shorter mean transit times in TNBC are in keeping with hyperdynamic blood flow in part due to blood shunting, with proportionally larger increases in blood flow relative to blood volume seen within this tumour type (MTT=BV/BF). Similarly, higher k_{ep} values in the TNBC group reflect the rapid return of contrast medium into the vasculature which is consistent with increased capillary permeability.

Given these differences in tumour vascular characteristics, anti-angiogenic therapy may be an appropriate targeted treatment for TNBC. There are a number of clinical trials currently addressing the benefit of anti-VEGF therapy in women with TNBC. So far, subset analyses of patients with triple-negative cancers in completed trials of bevacizumab in metastatic breast cancer have been encouraging, with the AVADO trial of bevacizumab (7.5 mg/kg vs 15 mg/kg), in addition to docetaxel in the first-line metastatic setting, demonstrating an improvement in PFS from 6.0 to 8.1 months (HR=0.60, 95% CI, 0.39–0.92) in the 15 mg/kg arm [35, 36]. In the E2100 trial, there were also improvements in PFS from 4.7 to 10.2 months (HR=0.45; 95% CI, 0.33–0.61) [37]. Subset analysis in RIBBON I, a phase III trial of bevacizumab in the first- and second-line treatment of metastatic breast cancer also showed improvements in PFS regardless of chemotherapy type (4.2 to 6.1 months in the capecitabine cohort (HR=0.72, 95% CI, 0.49–1.06); and from 8.2 to 14.5 months in the taxotere/anthracycline cohort (HR= 0.78, 95% CI, 0.53–1.15)), although these differences were not statistically significant [38]. Currently there are several studies assessing the role of bevacizumab in early TNBC including BEATRICE in the adjuvant setting and CALGB 40503 in the neoadjuvant setting.

Limitations

Given the limited study population and small patient numbers in each group, this study was not conducive to a multivariate analysis. We examined two subsets only; the triple-negative and ER+/PR+/HER2- groups as the latter

confers a better prognosis, and further studies comparing the triple-negative group with other breast cancers are needed. We recognise that although multiple statistical comparisons were performed in this analysis where the sample size was small this was an exploratory study designed to be hypothesis generating. However further validation in a larger patient population is warranted. To our knowledge, findings using fully quantitative methods of MRI kinetic analysis in contrast to semi-quantitative techniques such as enhancement kinetics [25, 39] have not been widely reported in the literature. A recent study demonstrated more rapid initial enhancement and higher washout rates in ER-/PR- breast cancers (as distinct from our defined subset of ER-/PR-/HER2- tumours); however like many studies, methods of data acquisition differed with longer temporal resolution times and no accounting for first pass effects [39].

Values for K^{trans}, a widely accepted DCE-MRI-derived measurement of perfusion and permeability, were not increased in TNBC in this study. However this transfer constant is not always an ideal parameter for reflecting vascularity. Any conditions influencing blood perfusion including patient factors such as cardiac output and hypertension which are difficult to control for in the clinical setting may potentially confound measurements of K^{trans}. k_{ep} on the other hand, provides a robust method of describing actual tumour capillary permeability because it is disconnected from perfusion. Although we appreciate that a mathematical relationship exists between k_{ep} and v_e: there is however, an underlying physiological justification for this. It is also important to mention that the compartmental pharmacokinetic modelling utilised in MRI analysis assumes that contrast agent resides and exchanges between two compartments, the vascular space and the EES, and hence may be an oversimplification of underlying tumour physiology.

Furthermore, triple-negative breast carcinomas are a heterogeneous subset of tumours and unlikely to represent a uniform entity [40]. Tumours were large in this study reflecting the neoadjuvant setting in which these patients were recruited. We recognise that although necrotic tumours may potentially influence our results, this was not the case in our study, but future studies incorporating pixel enhancement analysis and diffusion-weighted MRI may be of value in studying this further. Imaging studies investigating the underlying biological and functional features of these tumours will ultimately lead to an improved understanding of this subset of breast cancers. In particular, other multiparametric MRI techniques such as diffusion-weighted MRI which interrogates the extracellular space and intrinsic susceptibility-weighted MRI which can potentially inform on blood tumour oxygenation, may provide further information and reinforce our findings [41, 42].

Conclusions

In conclusion, the lower values of v_e and MTT, and higher k_{ep} in TNBC as elucidated by DCE-MRI, are in keeping with accumulating evidence that these tumours exhibit distinct underlying pathophysiological characteristics and clinical features in comparison with ER+/PR+/HER2- breast cancers. Dynamic MRI findings from our study were consistent with increased stromal cellular density and vascular permeability, suggesting that benefit may be gained from targeted therapies, in particular those directed at disrupting tumour angiogenesis.

References

1. Irvin WL Jr, Carey LA (2008) What is triple-negative breast cancer? Eur J Cancer 44:2799–2805

2. Bosch A, Erole P, Zaragoza R, Vina JR, Lluch A (2010) Triple-negative breast cancer: molecular features, pathogenesis, treatment and current lines of research. Cancer Treat Rev 36:206–215

3. Perou CM, Sorlie T, Eisen MB, van de Rijn M, Jeffrey SS, Rees CA, Pollack JR, Ross DT, Johnsen H, Akslen LA, Fluge O, Pergamenschikov A, Williams C, Zhu SX, Lonning PE, Borresen-Dale A-L, Brown PO, Botstein D (2000) Molecular portraits of human breast tumours. Nature 406:747–752

4. Sorlie T, Perou CM, Tibshirani R, Aas T, Geisler S, Johnsen H, Hastie T, Eisen MB, van de Rijn M, Jeffrey SS, Thorsen T, Quist H, Matese JC, Brown PO, Botstein D, Eystein Lønning P, Børresen-Dale AL (2001) Gene expression patterns of breast carcinomas distinguish tumor subclasses with clinical implications. Proc Natl Acad Sci USA 98:10869–10874

5. Rakha EA, Ellis IO (2009) Triple-negative/basal-like breast cancer: a review. Pathology 41(1):40–47

6. Kreike B, van de Vijver MJ (2007) Are triple-negative tumours and basal-like breast cancer synonymous? Breast Cancer Res 9:405

7. Collins DJ, Padhani AR (2004) Dynamic magnetic resonance imaging of tumor perfusion. Approaches and biomedical challenges. IEEE Eng Med Biol Mag 23:65–83

8. Chen JH, Agrawal G, Feig B, Baek HM, Carpenter PM, Mehta RS, Nalcioglu O, Su M-Y (2007) Triple-negative breast cancer: MRI features in 29 patients. Ann Oncol 18:2042–2043, Letters to the editor

9. Basu S, Chen W, Tchou J, Mavi A, Cermik T, Czerniecki B, Schnall M, Alavi A (2008) Comparison of triple-negative and estrogen receptor-positive/progesterone receptor-positive/HER2-negative breast carcinoma using quantitative fluorine-18 fluoro-deoxyglucose/positron emission tomography imaging parameters. Cancer 112:995–1000

10. Ah-See MW, Makris A, Taylor NJ, Harrison M, Richman PI, Burcombe RJ, Stirling JJ, d'Arcy JA, Collins DJ, Pittam MR, Ravichandran D, Padhani AR (2008) Early changes in functional dynamic magnetic resonance imaging predict for pathologic response to neoadjuvant chemotherapy in primary breast cancer. Clin Cancer Res 14:6580–6589

11. Sobin LH, Wittekind C (2002) TNM classification of malignant tumours. Wiley-Liss, UICC, New York

12. Bloom HJG, Richardson WW (1957) Histological grading and prognosis in breast cancer. Br J Cancer 11:359–377

13. Harvey JM, Clark GM, Osborne CK, Allred DC (1999) Estrogen receptor status by immunohistochemistry is superior to the ligand-binding assay for predicting response to adjuvant endocrine therapy in breast cancer. J Clin Oncol 17:1474–1481

14. Parker GJM, Suckling J, Tanner SF, Padhani AR, Revell PB, Husband JE, Leach MO (1997) Probing tumor microvascularity by measurement, analysis and display of contrast agent uptake kinetics. JMRI 7:564–574

15. Galbraith SM, Lodge MA, Taylor NJ, Rustin GJS, Bentzen S, Stirling JJ, Padhani AR (2002) Reproducibility of dynamic contrast-enhanced MRI in human muscles and tumours: comparison of quantitative and semi-quantitative analysis. NMR Biomed 15:132–142

16. d'Arcy JA, Collins DJ, Padhani AR, Walker-Samuel S, Suckling J, Leach MO (2006) Magnetic resonance imaging workbench (MRIW): dynamic contrast enhanced MRI data analysis and visualisation. Radiographics 26:621–632

17. Tofts PS, Berkowitz B, Schnall MD (1995) Quantitative analysis of dynamic Gd-DTPA enhancement in breast tumor using a permeability model. Magn Reson Med 33:564–568

18. Fritz-Hansen T, Rostrup E, Larsson HB, Sondergaard L, Ring P, Henriksen O (1996) Measurement of the arterial concentration of Gd-DTPA using MRI: a step toward quantitative perfusion imaging. Magn Reson Med 36:225–231

19. Walker-Samuel S, Leach MO, Collins DJ (2006) Evaluation of response to treatment using DCE-MRI: the relationship between initial area under the gadolinium curve (IAUGC) and quantitative pharmacokinetic analysis. Phys Med Biol 51:3593–3602

20. Walker-Samuel S, Parker C, Leach MO, Collins DJ (2007) Reproducibility of reference tissue quantification of dynamic contrast-enhanced data: comparison with a fixed vascular input function. Phys Med Biol 52:75–89

21. Livasy CA, Karaca G, Nanda R, Tretiakova MS, Olopade OI, Moore DT, Perou CM (2006) Phenotypic evaluation of the basal-like subtype of invasive breast carcinoma. Mod Pathol 19:264–271

22. Fulford LG, Easton DF, Reis-Filho JS, Sofronis A, Gillett CE, Lakhani SR, Hanby A (2006) Specific morphological features predictive for the basal phenotype in grade 3 invasive ductal carcinoma of the breast. Histopathology 49:22–34

23. Gluz O, Liedtke C, Gottschalk N, Pusztai L, Nitz U, Harbeck N (2009) Triple-negative breast cancer-current status and future directions. Ann Oncol 20:1913–1927

24. Ko ES, Lee BH, Kim HA, Noh WC, Kim MS, Lee SA (2010) Triple-negative breast cancer: correlation between imaging and pathological findings. Eur Radiol 20:1111–1117

25. Uematsu T, Kasami M, Yuen S (2009) Triple-negative breast cancer: correlation between MR imaging and pathologic findings. Radiology 250:638–647

26. Tchou J, Wang L-P, Sargen M, Sonnad S, Tomaszewski J, Schnall M (2006) Do triple-negative breast cancers have a distinct imaging phenotype? [abstract]. Breast Cancer Res Treat 100:s128

27. Miles KA, Williams RE (2008) Warburg revisited: imaging tumour blood flow and metabolism. Cancer Imaging 8:81–86

28. Bergamaschi A, Tagliabue E, Sorlie T, Naume B, Triulzi T, Orlandi R, Russnes HG, Nesland JM, Tammi R, Auvinen P, Kosma VM, Ménard S, Borresen-Dale AL (2008) Extracellular matrix signature identified breast cancer subgroups with different clinical outcome. J Pathol 214:357–367

29. Foulkes WD, Brunet JS, Stefansson IM, Straume O, Chappuis PO, Begin LR, Hamel N, Goffin JR, Wong N, Trudel M, Kapusta L, Porter P, Akslen LA (2004) The prognostic implication of the basal-like (cyclin E high/p27 low/p53+/glomeruloid-microvascular

proliferation+) phenotype of BRCA1-related breast cancer. Cancer Res 64:830–835

30. Linderholm BK, Hellborg H, Johansson U, Ellmberger G, Skoog L, Lehtio J, Lewensohn R (2009) Significantly higher levels of vascular endothelial growth factor (VEGF) and shorter survival times for patients with primary operable triple-negative breast cancer. Ann Oncol 20:1639–1646

31. Linderholm BK, Lindahl T, Holmberg L, Klaar S, Lennerstrand J, Henriksson R, Bergh J (2001) The expression of vascular endothelial growth factor correlates with mutant p53 and poor prognosis in human breast cancer. Cancer Res 61:5407–5414

32. Greenberg A, Rugo HS (2010) Triple-negative breast cancer: role of antiangiogenic agents. Cancer J 16:33–38

33. Shi YH, Bingle L, Gong LH, Wang YX, Corke KP, Fang WG (2007) Basic FGF augments hypoxia induced HIF-1 alpha expression and VEGF release in T47D breast cancer cells. Pathology 39:396–400

34. Raghunand N, Gatenby RA, Gillies RJ (2003) Microenvironmental and cellular consequences of altered blood flow in tumours. Br J Radiol 76:S11–S22

35. Miles D, Chan A, Romieu G, Dirix LY, Cortes J, Pivot X, Tomczak P, Juozaityte E, Harbeck N, Steger GG, the BO17708 Study Group (2009) Randomized, double-blind, placebo-controlled, phase III study of bevacizumab with docetaxel or docetaxel with placebo as first-line therapy for patients with locally recurrent or metastatic breast cancer (mBC) [abstract]. 32nd San Antonio Breast Cancer Symposium. Available at http://www.sabcs.org/Newsletter/Docs/SABCS_2009_Issue1.pdf. Accessed 23.9.2010

36. O'Shaughnessy J, Dieras V, Glaspy J, Brufsky A, Miller K, Miles D, Koralewski P, Phan S, Bhattacharya S (2009) Comparison of subgroup analyses of PFS from three phase II studies of bevacizumab in combination with chemotherapy in patients with HER2-negative metastatic breast cancer (MBC) [abstract]. Cancer Res 69:s207

37. Miller K, Wang M, Gralow J, Dickler M, Cobleigh M, Perez EA, Shenkier T, Cella D, Davidson NE (2007) Paclitaxel plus bevacizumab versus paclitaxel alone for metastatic breast cancer. N Engl J Med 357:2666–2676

38. Robert N, Dieras V, Glaspy J, Brufsky A, Bondarenko I, Lipatov O, Perez E, Yardley D, Phan S, Bhattacharya S, O'Shaughnessy J (2009) Clinical benefit rate and time to response in RIBBON-1, a randomized, double-blind, phase III trial of chemotherapy with or without bevacizumab (B) for the first-line treatment of HER2-negative locally recurrent or metastatic breast cancer (MBC) [abstract]. Cancer Res 69:s6084

39. Baltzer PA, Vag T, Dietzel M, Beger S, Freiberg C, Gajda M, Camara O, Kaiser WA (2010) Computer-aided interpretation of dynamic magnetic resonance imaging reflects histopathology of invasive breast cancer. Eur Radiol 20(1):563–571

40. Dawson SJ, Provenzano E, Caldas C (2009) Triple negative breast cancers: clinical and prognostic implications. Eur J Cancer 45:27–40

41. Padhani AR, Liu G, Koh DM, Chenevert TL, Thoeny HC, Takahara T, Dzik-Jurasz A, Ross BD, Van Cauteren M, Collins D, Hammoud DA, Rustin GJ, Taouli B, Choyke PL (2009) Diffusion-weighted magnetic resonance imaging as a cancer biomarker: consensus and recommendations. Neoplasia 11:102–125

42. Li SP, Taylor NJ, Makris A, Ah-See ML, Beresford MJ, Stirling JJ, d'Arcy JA, Collins DJ, Padhani AR (2010) Primary human breast adenocarcinoma: imaging and histologic correlates of intrinsic susceptibility-weighted MR imaging before and during chemotherapy. Radiology 257:643–652, Epub 2010 Sep 21